Magnetic Resonance in an Atomic Vapor Excited by a Mechanical Resonator

Ying-Ju Wang,[1] Matthew Eardley,[1,3] Svenja Knappe,[1] John Moreland,[2] Leo Hollberg,[1] and John Kitching[1]

[1]*Time and Frequency Division, National Institute of Standards and Technology, 325 Broadway, Boulder, Colorado 80305, USA*
[2]*Electromagnetics Division, National Institute of Standards and Technology, 325 Broadway, Boulder, Colorado 80305, USA*
[3]*Department of Physics and Astronomy, SUNY Stony Brook, Stony Brook, New York 11794, USA*
(Received 24 May 2006; published 1 December 2006)

We demonstrate a direct resonant interaction between the mechanical motion of a mesoscopic resonator and the spin degrees of freedom of a sample of neutral atoms in the gas phase. This coupling, mediated by a magnetic particle attached to the tip of the miniature mechanical resonator, excites a coherent precession of the atomic spins about a static magnetic field. The novel coupled atom-resonator system may enable development of low-power, high-performance sensors, and enhance research efforts connected with the manipulation of cold atoms, quantum control, and high-resolution microscopy.

In this experiment, magnetic resonance is observed in a miniature atomic vapor cell by using a microfabricated cantilever to drive coherent precession of the net atomic polarization. The observed resonance is evidence of direct coupling between the motion of a mechanical resonator and the spin degrees of freedom of neutral alkali atoms in the gas phase. The coupling of resonant mechanical microstructures to atoms or molecules in solid state or liquid systems has played a critical role in advancements of scanning probe microscopy since the 1980s [1–3]. High force sensitivity to single electron spins has been projected [4] and demonstrated [5] with a magnetic resonance force microscope [6]. While the large quality factors of cantilevers give high detection sensitivities, their localized interaction with the sample surface also leads to fine spatial resolution. The high quality factors also enable potential application to low-power devices by integrating magnetic cantilevers with semiconductor-based components. For instance, to reduce power consumption, one can imagine the use of oscillating magnetic cantilevers as a low-power rf source in chip-scale atomic devices [7,8]. In addition, if strong coupling between a magnetic cantilever and atomic spins could be achieved, stimulated amplification of mechanical motion of the resonators could occur, leading to the possibility of a "mechanical laser" [9].

Achieving long coherence times is essential for high-fidelity manipulation and probing of the spin polarization of atoms, particularly near the quantum limit. Long spin relaxation times of solid state samples are often achieved by cryogenic cooling to reduce thermally induced magnetic noise and by increasing the magnetic field gradient at the sample to suppress spin diffusion [10]. Alternatively, the coherence time can be increased through the use of a more dilute sample, such as an atomic vapor, in which the interparticle interactions are weaker.

As a first step toward combining the advantages of resonant microstructures and atomic vapor samples, we demonstrate here the coupling between a mechanical resonator and atoms in the gas phase. Our approach uses a microfabricated cantilever with a magnetic tip to drive a magnetic resonance of neutral alkali atoms confined in a microfabricated vapor cell above room temperature. We discuss the effects of diffusion in the inhomogeneous static and rf fields on the spin relaxation, which determine the linewidth of the magnetic resonance. We also evaluate the magnetic field sensitivity of such a system operated as a magnetic field sensor.

In the experiment, shown schematically in Fig. 1, a circularly polarized light field is incident on a sample of neutral alkali atoms in the gas phase. If the external magnetic field is weak, the spin of the valence electron is strongly coupled to the nuclear spin by the hyperfine interaction and the resulting "atomic" spin can be polar-
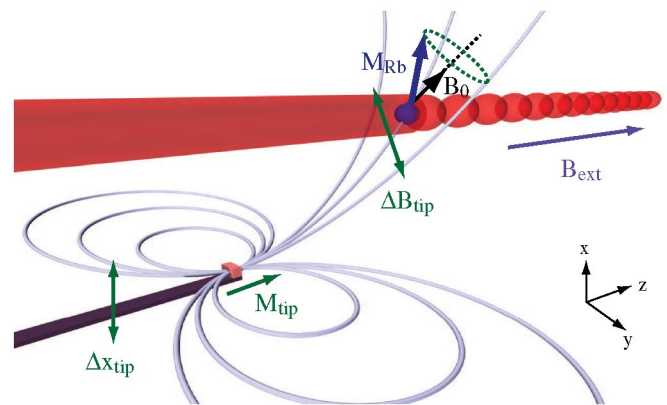

FIG. 1 (color online). The cantilever tip has a magnetic moment $\vec{M}_{\text{tip}}$. The motion (Δx_{tip}) of the tip of a microfabricated cantilever creates an oscillatory magnetic field ($\Delta \vec{B}_{\text{tip}}$) at the location of the atomic sample, which excites a coherent precession of the atomic spin about a static magnetic field $\vec{B}_0$. The resulting time-varying precession is detected through the intensity modulation it creates on a resonant, circularly polarized optical field. The total static magnetic field is a combination of the dc field produced by the cantilever tip and an applied field ($\vec{B}_{\text{ext}}$).

ized along the direction of propagation of the light field. The resulting magnetic moments (M_{Rb}) of the Rb atoms are dominated by the electron magnetic moment and precess along the static field at the Larmor frequency $\omega = \gamma|\vec{B}_0|$, where $\gamma = 2\pi \times 7$ Hz/nT is the gyromagnetic ratio of the ^{87}Rb atoms. The oscillatory magnetic field created by the motion of the cantilever tip drives the atomic spin precession coherently and a change or modulation in the optical absorption is then produced that has a well-defined phase relation to the cantilever motion. The modulated absorption is detected by the same laser beam used to optically pump the atoms.

The experimental arrangement consists of a miniature alkali vapor cell placed near a cantilever with a magnetic tip. The cell and cantilever are surrounded by a single-layer magnetic shield, which reduces the effects of Earth's and laboratory magnetic fields. A static magnetic bias field $\vec{B}_{ext}$ oriented along the axis of the cantilever (z axis) is generated by a solenoid inside the shield. The setup is placed inside a vacuum chamber to reduce viscous damping of the cantilever motion by air molecules which would otherwise decrease the quality factor of the mechanical resonance. The cell, similar to the one in Ref. [11], is cubic with an interior volume of 1 mm^3 and contains a thermal vapor of ^{87}Rb along with a buffer gas mixture of Ar and Ne with pressures of 5 and 31 kPa at room temperature, respectively. The buffer gas is added to reduce the rate of decoherence due to collisions with the cell walls. The cell is heated to ~130 °C to increase the density of alkali atoms and the optical absorption. The cantilever has dimensions of 3 μm(x) $\times$ 30 μm(y) $\times$ 220 μm(z) and is mounted on a piezoelectric transducer (PZT) and placed adjacent to the vapor cell. The cantilever is located on the same horizontal plane as the bottom of the cell. The axis of the cantilever points toward to the cell but is offset from the center vertically.

As shown in Fig. 2, a magnetic particle of NdFeNbB is attached to the tip of the cantilever. The magnetic particle has dimensions of roughly 10 μm $\times$ 50 μm $\times$ 100 μm and a magnetic moment on the order of 10^{-9} A $\cdot$ m^2 oriented along the axis of the cantilever (z direction). The field generated in the cell by the magnetic tip can be approximated as that produced by a magnetic dipole, which strongly diverges as a function of the distance from the tip. The tip therefore produces a magnetic field with both dc ($\vec{B}_{tip}$) and oscillatory components ($\Delta\vec{B}_{tip}$)
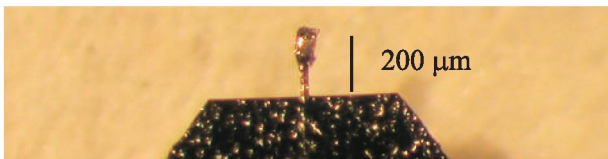

FIG. 2 (color online). The magnetic cantilever. A small magnetic particle of NdFeNbB is attached to the tip of the cantilever to produce a magnetic field.

within the atomic sample when the frequency of the PZT driving signal is equal to the mechanical resonant frequency of the cantilever.

The laser beam used to pump and probe the atomic spins is produced by a vertical-cavity surface-emitting laser (VCSEL) at 795 nm. The diameter of the beam is about 1 mm, and the optical power is 10 μW measured after the cell when the optical frequency is tuned off atomic resonance. The laser is circularly polarized, and its frequency is locked precisely to the D1 ($5S_{1/2} \rightarrow 5P_{1/2}$) transition of ^{87}Rb with a second vapor cell. The laser optically pumps the atoms into a longitudinally polarized "dark state" so that the optical absorption is reduced. Motion of the cantilever tip creates an oscillatory field ($\Delta\vec{B}_{tip}$) with a component perpendicular to the direction of the total magnetic field, which is a combination of the bias magnetic field produced by the external coil and the tip of the cantilever ($\vec{B}_0 = \vec{B}_{ext} + \vec{B}_{tip}$). Resonance is established locally within the cell when $2\pi f_{osc} = \gamma|\vec{B}_0|$, where f_{osc} is the frequency of the oscillatory field. Under the resonance condition, a change or modulation of the absorption signal is detected, depending on the orientation of the optical axis with respect to $\vec{B}_0$ [12–14]. Because $\vec{B}_{tip}$ is strongly divergent, the direction of the total field $\vec{B}_0$ is not in general parallel to the propagation direction of the optical beam, and a modulation signal is observed in addition to the dc change in absorption. A plot of the estimated field strength in the cell is shown in Fig. 3. We selectively observe the absorption signal at the drive frequency using lock-in detection with the PZT input signal as reference.

The magnetic resonance signal, shown in Fig. 4, is the in-phase component of the lock-in output observed when the frequency of the PZT drive is swept at a rate of 200 Hz/s with a time constant of the lock-in at 1 ms. The graph in Fig. 4(a) shows that the magnetic resonance consists of two components: a broad background with a width of about 15 kHz, and a narrow signal with a width of about 9 Hz at the cantilever resonant frequency. The back-
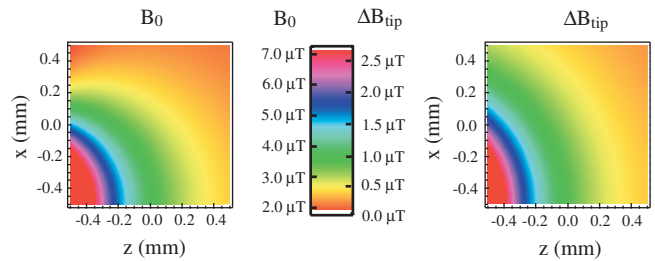

FIG. 3 (color online). A two-dimensional contour plot of $\vec{B}_0$ and $\Delta\vec{B}_{tip}$, slicing through the cell center plane. The model assumes that the magnetic dipole (the tip) is 3.25×10^{-9} A $\cdot$ m^2 at $(x, z) = (-0.5$ mm, -1.0 mm$)$, $B_{ext} = 1.8$ μT, and the cell center is at the origin. The tip displacement used to calculate the rf field $\Delta\vec{B}_{tip}$ is assumed to be 200 μm and is estimated from the PZT displacement enhanced by the Q factor of the cantilever.

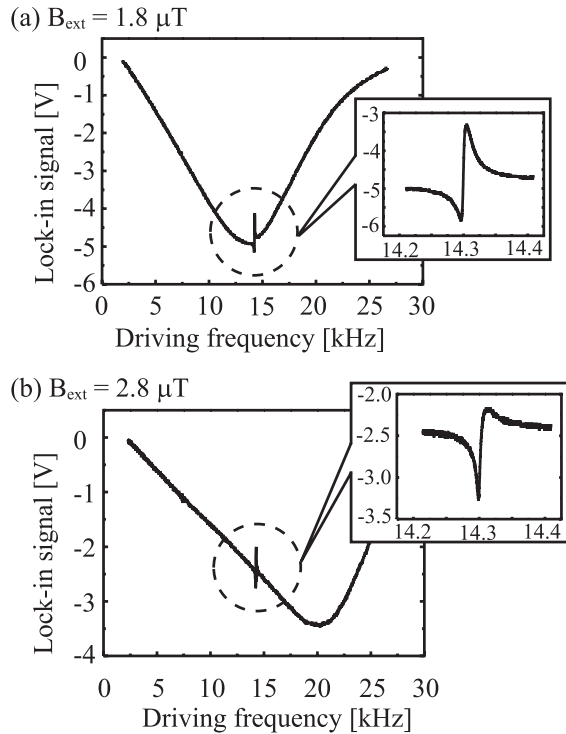(a) $B_{ext} = 1.8$ μT

(b) $B_{ext} = 2.8$ μT

FIG. 4. The magnetic resonances. (a) $|\vec{B}_{ext}| = 1.8$ μT: the center frequency of the broad resonance is at the vibrational frequency of the cantilever. (b) $|\vec{B}_{ext}| = 2.8$ μT: the center frequency of the broad resonance is offset from the vibrational frequency of the cantilever. The insets show the narrow resonances at a reduced span and sweep rate of the driving frequency.

ground signal is the magnetic resonance excited by the oscillatory magnetic field that is produced by the driving current flowing into the PZT. The peak of this broad resonance roughly equals the mean precession frequency of the atoms that is primarily determined by the static field; the peak therefore shifts when we adjust the external bias field, as shown in Fig. 4(b). The inset in Fig. 4(a) shows the narrow resonance at a reduced span and sweep rate (20 Hz/s) of the driving frequency. The peak position coincides with the mechanical resonance of the cantilever and is largely independent of the external bias field, as shown in the inset in Fig. 4(b). These observations show that the feature is due to the motion of the cantilever and not due to effects related to the field inhomogeneity [15,16]. Because the cantilever has a relatively high mechanical Q factor (~ 1000), its motion is small when the drive frequency is far from its resonance frequency and therefore the oscillating field it creates is negligible. The narrow resonance has a dispersive profile as opposed to the absorptive profile of the broad resonance. Dispersive phase shifts are expected at mechanical resonance. In addition, this difference could be due to the spatial correlation between the inhomogeneous static and the rf field produced by the cantilever as described in Refs. [15,16].

Though not the primary focus of this work, we studied the amplitude dependence of the magnetic resonance sig-

nal driven by the cantilever as a function of the external bias field, which served as a useful diagnostic for using this coupled cantilever-atom system as a magnetometer. The amplitude of the narrow resonance depends on the mean precession frequency of the atoms, i.e., the external bias field. The peak-to-peak amplitude as measured by lock-in detection is plotted as a function of external bias field in Fig. 5. From the data and a measurement of the noise of the optical readout (4.6 mV/$\sqrt{Hz}$), we establish that the magnetic field sensitivity of the present configuration is on the order of 10 nT/$\sqrt{Hz}$ at 1 Hz.

The overall sensitivity to magnetic fields is limited by the broad linewidth due to spin relaxation. The inhomogeneous broadening of the precession frequency from the nonuniform static field is about 4 kHz full width at half maximum, which is considerably less than the observed broadening. Because of the strong inhomogeneity of both the static and rf fields in our experiment, spin relaxation due to diffusion must be considered to account for the linewidth. The diffusion of atoms in an inhomogeneous static field results in spin relaxation as is well known from many nuclear magnetic resonance (NMR) experiments since the 1950s [17–19]. Inhomogeneous rf fields also cause linewidth broadening in atomic systems whose magnetic moment is dominated by the electron spin, as demonstrated in earlier work [16].

The spatial distribution of the magnetic polarization can be characterized by a dephasing length, which is the average length a spin travels before acquiring a phase shift of approximately π. For the given average static field gradient g (6 μT/cm) and diffusion constant D (0.65 cm^2/s [20] for the buffer gases used here), the dephasing length is estimated as $l_g \approx (D/\gamma g)^{1/3} \approx 140$ μm [21,22]. The dephasing length is smaller than the cell size, so most of the atoms lose their coherence before they collide with the cell walls. Because of the field gradient, only a fraction of atoms in the cell, i.e., the ones in the "resonant slice"
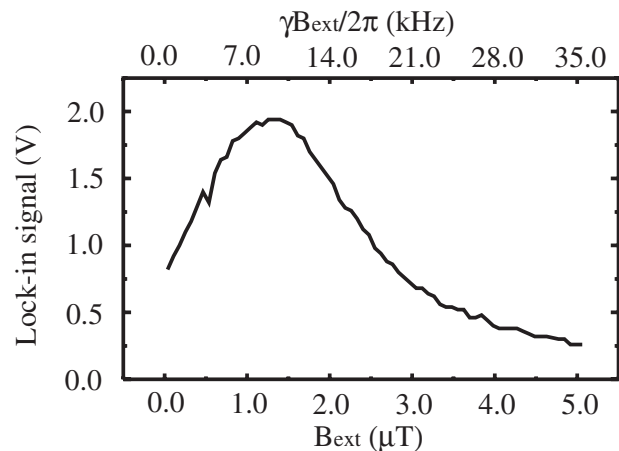

FIG. 5. The amplitude of the magnetic resonance driven by the cantilever as a function of the external magnetic field.

defined by the resonance condition and dephasing length, interact with the cantilever for a given bias field. We conclude that the amplitude of the magnetometer signal is therefore relatively small compared to that would be observed in a homogeneous field.

This system could be optimized and improved for application as a magnetic field sensor in several ways. The field inhomogeneity can be reduced while maintaining relatively large transverse oscillating fields through the use of a cantilever with a more appropriate design. For example, one could use a torsional cantilever [23–25] with dual magnets oriented perpendicular to the rotation axis to produce a more uniform field. The oscillating field strength of a torsional cantilever is determined by the amplitude of the angular motion but is independent of the field gradient. A larger magnetic resonance signal could also be achieved by increasing the volume of the tip magnet to create a larger magnetic moment and stronger rf field for a given distance between the cantilever and the atoms. Nevertheless, the results here clearly demonstrate that direct coupling between a mechanical resonator and atomic spins in the vapor can be detected with excellent signal to noise even in the presence of a strong field gradients. In addition, spin coherence times of atoms in the gas phase can be quite long, of the order of milliseconds even in millimeter-scale cells at room temperature, which is encouraging for future applications.

From another perspective, large field gradients are an advantage for some purposes. The coupling between the magnetic moment of the atoms and the magnetic cantilever described here could be used to provide highly localized excitations for coherent manipulation of spins of laser-cooled, trapped atoms. For example, cold atoms in a certain quantum states could be magnetically trapped in the potential produced by the tip field-gradient in the presence of an opposing uniform magnetic field [26]. In this case, small cantilevers with strong field gradients should produce a highly localized sample of atoms trapped very near the tip and strongly coupled to its mechanical motion. We can even envision arrays of magnetic cantilevers coupled to each other through their mechanical motion, each component of which could be coupled to an atomic ensemble through its respective magnetic moment. Such systems may prove useful in quantum computation [27], for probing or manipulating the internal state of a single ion or atom. We note that related systems have been considered in the context of trapped ions [27,28] and cryogenically cooled Josephson junctions [29,30].

[1] G. Binnig, C. F. Quate, and C. Gerber, Phys. Rev. Lett. **56**, 930 (1986).

[2] Y. Martin and H. K. Wickramasinghe, Appl. Phys. Lett. **50**, 1455 (1987).

[3] J. J. Sáenz, N. García, P. Grütter, E. Meyer, H. Heinzelmann, R. Wiesendanger, L. Rosenthaler, H. R. Hidber, and H.-J. Güntherodt, J. Appl. Phys. **62**, 4293 (1987).

[4] J. A. Sidles, J. L. Garbini, K. J. Bruland, D. Rugar, O. Züger, S. Hoen, and C. S. Yannoni, Rev. Mod. Phys. **67**, 249 (1995).

[5] D. Rugar, R. Budakian, H. J. Mamin, and B. W. Chui, Nature (London) **430**, 329 (2004).

[6] J. A. Sidles, Appl. Phys. Lett. **58**, 2854 (1991).

[7] S. Knappe, V. Shah, P. D. D. Schwindt, L. Hollberg, J. Kitching, L.-A. Liew, and J. Moreland, Appl. Phys. Lett. **85**, 1460 (2004).

[8] V. Shal, L. Hollberg, P. D. D. Schwindt, S. Knappe, J. Kitching, L.-A. Liew, and J. Moreland, Appl. Phys. Lett. **85**, 6409 (2004).

[9] I. Bargatin and M. L. Roukes, Phys. Rev. Lett. **91**, 138302 (2003).

[10] R. Budakian, H. J. Mamin, and D. Rugar, Phys. Rev. Lett. **92**, 037205 (2004).

[11] L. Liew, S. Knappe, J. Moreland, H. Robinson, L. Hollberg, and J. Kitching, Appl. Phys. Lett. **84**, 2694 (2004).

[12] H. G. Dehmelt, Phys. Rev. **105**, 1487 (1957).

[13] W. E. Bell and A. L. Bloom, Phys. Rev. **107**, 1559 (1957).

[14] A. L. Bloom, Appl. Opt. **1**, 61 (1962).

[15] R. Barbé, M. Leduc, and F. Laloë, J. Phys. (Paris) **35**, 699 (1974).

[16] R. Barbé, M. Leduc, and F. Laloë, J. Phys. (Paris) **35**, 935 (1974).

[17] H. C. Torrey, Phys. Rev. **92**, 962 (1953).

[18] H. Y. Carr and E. M. Purcell, Phys. Rev. **94**, 630 (1954).

[19] H. C. Torrey, Phys. Rev. **104**, 563 (1956).

[20] W. Franzen, Phys. Rev. **115**, 850 (1959).

[21] M. D. Hurlimann, K. G. Helmer, T. M. Deswiet, and P. N. Sen, J. Magn. Reson., Ser. A **113**, 260 (1995).

[22] T. M. de Swiet and P. N. Sen, J. Chem. Phys. **100**, 5597 (1994).

[23] R. N. Kleiman, R. N. Kleiman, G. K. Kaminsky, J. D. Reppy, R. Pindak, and D. J. Bishop, Rev. Sci. Instrum. **56**, 2088 (1985).

[24] P. Rösner, K. Samwer, R. O. Pohl, and S. Schneider, Rev. Sci. Instrum. **74**, 3395 (2003).

[25] M. D. Chabot and J. Moreland, J. Appl. Phys. **93**, 7897 (2003).

[26] V. Vuletic, T. Fischer, M. Praeger, T. W. Hänsch, and C. Zimmermann, Phys. Rev. Lett. **80**, 1634 (1998).

[27] D. J. Wineland, C. Monroe, W. M. Itano, D. Leibfried, B. E. King, and D. M. Meekhof, J. Res. Natl. Inst. Stand. Technol. **103**, 259 (1998).

[28] W. K. Hensinger, D. W. Utami, H.-S. Goan, K. Schwab, C. Monroe, and G. J. Milburn, Phys. Rev. A **72**, 041405(R) (2005).

[29] E. K. Irish and K. Schwab, Phys. Rev. B **68**, 155311 (2003).

[30] E. K. Irish, J. Gea-Banacloche, I. Martin, and K. C. Schwab, Phys. Rev. B **72**, 195410 (2005).